Multilayer mirror and foil filter AXUV diode arrays on CDX-U spherical torus

V. A. Soukhanovskii,[a] D. Stutman, M. Iovea, M. Finkenthal,[b] and H. W. Moos
Plasma Spectroscopy Group, Department of Physics and Astronomy, The Johns Hopkins University, Baltimore, Maryland 21218

T. Munsat, B. Jones, D. Hoffman, R. Kaita, and R. Majeski
Princeton Plasma Physics Laboratory, Princeton University, Princeton, New Jersey 08543

(Presented on 20 June 2000)

Recent upgrades to CDX-U spherical torus diagnostics include two 10-channel AXUV diode arrays. The multilayer mirror (MLM) array measures the λ150 O VI brightness profile in the poloidal plane using the Mo/B_4C synthetic multilayer structures as dispersive elements. The foil filter array has a tangential view and is equipped with interchangeable clear aperture, beryllium and titanium filters. This allows measurements of radiated power, O VI or C V radial distributions, respectively. The O VI and C V emissivity and the radiated power profiles are highly peaked. A Neoclassical impurity accumulation mechanism is considered as an explanation. For radiated power measurements in the $T_e \leqslant 100$ eV plasmas, photon energy dependent corrections must be used in order to account for nonlinear AXUV sensitivity in the range $E_{phot} \leqslant 20$ eV. The arrays are also used for characterization of resistive MHD phenomena, such as the low m modes, saw-tooth oscillations and internal reconnection events. Based on the successful operation of the diagnostics, a new ultra soft x-ray multilayer mirror diode AXUV diode array monitoring the 34 Å emissivity distribution of C VI will be built and installed on the National Spherical Torus Experiment. © *2001 American Institute of Physics.* [DOI: 10.1063/1.1323254]

I. INTRODUCTION

Multi-channel x-ray or vacuum ultraviolet (VUV) diagnostics are commonly used on most high temperature fusion plasma devices (in particular, tokamaks) for plasma imaging, impurity transport and magneto-hydrodynamic (MHD) instability studies. Recent progress in silicon semiconductor detector technology stimulated the development of absolute Si photodiodes.[1] These detectors, hereforth referred to as AXUV diodes, have linear response in a wide dynamic range, an average 0.25 A/W sensitivity for photons in the energy range $1 \leqslant E_{phot} \leqslant 7000$ eV and the time response on the order of 1 μs. They are also insensitive to neutral particles. These properties make them very attractive for observations of MHD oscillations, radiated power measurements and imaging of fast radiative phenomena.[2,3] In this paper, we demonstrate how low-cost AXUV diode arrays can be effectively used in a small scale plasma experiment for radiated power and impurity density profile measurements, from which Z_{eff} and impurity transport are derived. Design and operation of two AXUV diode arrays on the CDX-U spherical torus at Princeton Plasma Physics Laboratory are described. The principle of operation and some relevant details of the design are also discussed in Refs. 4 and 5. The arrays were built as prototypes of the multichannel ultrasoft x-ray imaging system[6] for the NSTX spherical torus. On CDX-U, one array is used for O VI λ150 emissivity measurements, and another is used for radiated power measurements and soft x-ray and extreme ultraviolet (XUV) plasma imaging. We point out that utilization of AXUV diodes as radiometers for plasmas with electron temperature $T_e \leqslant 100$ eV, typical of the edge or divertor plasmas in large tokamaks, may lead to underestimating the radiated power. A significant fraction of radiated power in such plasmas is due to line emission of lower charge states of low Z impurities, in the spectral range $5 \leqslant E_{phot} \leqslant 15$ eV. The AXUV diodes sensitivity is variable in this range (Fig. 1). Thus, photon energy dependent corrections must be applied to recover the true radiated power.

CDX-U is a small spherical torus ($R = 0.35$ m, $a = 0.22$ m, $B_{tor} = 0.23$ T) with the following typical plasma parameters: $T_e \leqslant 100$ eV, $n_e \leqslant 2 \times 10^{13}$ cm^{-3}, and the discharge flat-top of about 5 ms. The research has recently focused on

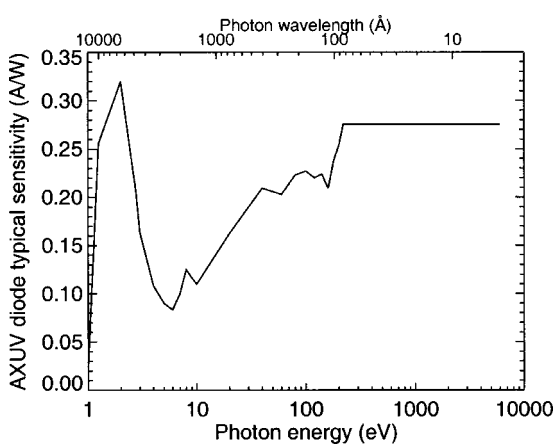

FIG. 1. Typical sensitivity of the AXUV diode.

[a]Present address: Princeton Plasma Physics Laboratory, Princeton, New Jersey 08543.
[b]Permanent address: Racah Institute of Physics, The Hebrew University, Jerusalem, Israel.

 © 2001 American Institute of Physics

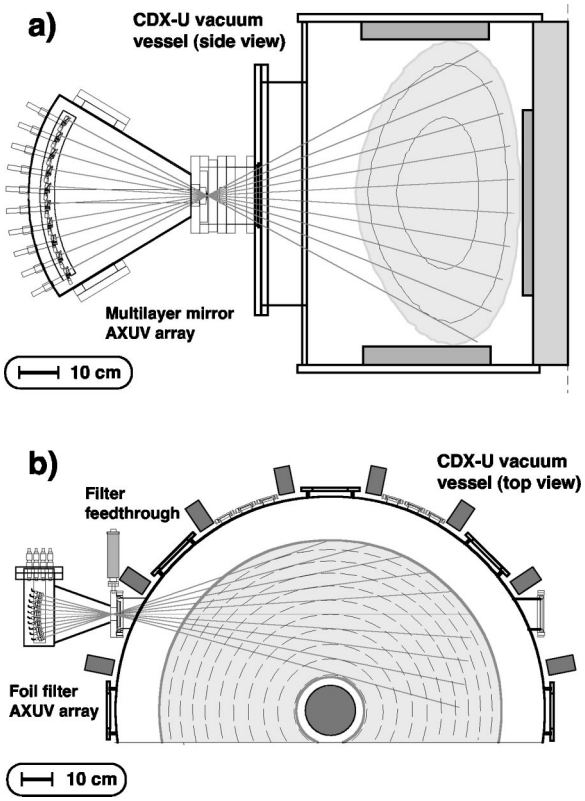

FIG. 2. Layout and placement of the multilayer mirror (a) and the foil filter and radiometer (b) AXUV diode arrays. Also shown are the simulated lines of sight and magnetic flux surfaces.

spherical tori (ST) physics, high harmonic fast wave (HHFW) plasma heating, electron Bernstein wave (EBW) detection and impurity transport.[7–11] Electron temperature in CDX-U is measured by a multipoint Thomson scattering system.[12] Electron density is measured by a microwave interferometer.[13] A triple Langmuir probe is used for the edge T_e and n_e measurements. Other diagnostics include a Rogowski coil, Mirnov pickup coils[14] and an EBW radiometer for T_e measurements.[15] Spectroscopic diagnostics comprises an extensive set of various soft x-ray (SXR), vacuum ultraviolet (VUV) and visible instruments.[11] Major intrinsic impurities in CDX-U are carbon and oxygen. The spectroscopy monitors C V and O VI brightness profiles, characteristic of the plasma core ($r/a \leqslant 0.3$), and C III, C IV, and O II lines from the plasma periphery. Of interest to further discussion, a 30-channel foil filter Si surface barrier diode (SBD) array,[4,14] equipped with interchangeable 3 kÅ foil Ti or a 5 kÅ foil Be filters, is used for imaging of predominantly C V and O VI emission in the poloidal plane. Throughout the paper, the units of Å are used for wavelengths, and emissivities are expressed in photon units unless noted otherwise.

II. AXUV DIODE ARRAYS ON CDX-U

A. Multilayer mirror array

The 10-channel multilayer mirror (MLM) array is mounted on the CDX-U mid-plane 8″ port [Fig. 2(a)]. The array is enclosed in a custom welded ultra high vacuum stainless steel chamber. Each channel represents a miniature MLM monochromator, which consists of a dispersive element — the MLM — in a rotatable holder and an AXUV diode (Sec. II C). A 5 kÅ Be foil filter, mounted on the central aperture of 1.375 cm$\times$1.0 cm, is used to block the visible, UV and VUV radiation. Constructive interference of a synthetic multilayer structure is described by the Bragg equation $n\lambda = 2d \sin\theta$, where d is the layer thickness, θ is the angle of incidence, and n is the spectral order used. The λ150 O VI resonant line ($2s\,^2S - 3p\,^2P$) is chosen because it is bright and isolated. The Mo/B_4C mirrors from Ovonics, Inc. with $2d = 187.4$ Å and the number of layers $N = 75$ are used. The MLM properties determine the monochromator spectral resolution: $\lambda/\Delta\lambda \simeq nN$. For the Mo/$B_4$C mirrors, the theoretical spectral bandpass is $\Delta\lambda \simeq 2$ Å, whereas the measured spectral bandpass is about 7 Å.[16] The mirrors were cut from one wafer. The measured wafer reflectivity is $R \simeq 0.27$ at $\lambda = 150$ Å, and $R \geqslant 0.20$ in the range 90–180 Å.[16] Due to surface quality and layer thickness variations across the wafer, the reflectivity variation from mirror to mirror is conservatively estimated to be up to 5%. Optical alignment of the $\theta - 2\theta$ mirror-detector geometry was performed with a HeNe laser for each monochromator. The angle θ corresponding to the wavelength λ150 was calculated using the measured $2d$ value: $2d = 180.8 \pm 4.9$ Å.[16] The θ value is $56.1° \pm 2.6°$, which corresponds to $\Delta\lambda \simeq 4$ Å. The angles were set using a removable mechanical rotation stage, with the estimated accuracy of $\pm 1°$. The etendue of each monochromator is 8×10^{-4} cm^2 sr. The wavelength range accepted by the collimator is $\lambda = 150.1 \pm 1.2$ Å.

Invoking the assumption that impurity ions are distributed uniformly over the magnetic flux surfaces, the D-shaped poloidal cross-section flux contours are approximated by elliptic contours, which are not necessarily concentric in the vertical or horizontal direction.[5] By means of the linear transformations described in Refs. 17 and 18, the ellipses are transformed into the circular coordinate system, and the line integrated brightnesses (irradiances) measured by each MLM array channel are corrected accordingly. The λ150 O VI line emissivity profile is obtained by the Abel inversion.

A 1 m grazing incidence extreme ultraviolet (XUV) space and time resolving spectrometer (STRS) with a radial mid-plane line of sight is used to ascertain the spectral purity of the emission within the MLM bandpass $\Delta\lambda$, and within the filter transmission bandpass of the foil filter array. At present, the spectrometer is equipped with a gold coated 2400 lines/mm grating and a photometrically uncalibrated detector, consisting of a chevron micro-channel plate (MCP), P20 phosphor and a Princeton Instruments MicroMax CCD camera, mechanically shuttered for 10 ms of the discharge. Shown in Fig. 3 are the impurity XUV spectra from a standard discharge (a) and a titanium contaminated discharge (b). Titanium gettering is used between discharges on CDX-U for intrinsic impurity content reduction. Also shown is the MLM reflectivity bandpass.

B. Foil filter and radiometer array

The schematic of the 10-channel foil filter and radiometer (FFR) array with a tangential mid-plane view of the

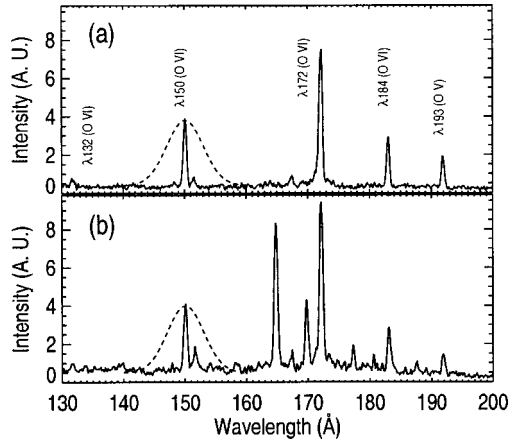

FIG. 3. Impurity spectra recorded by the STRS grazing incidence spectrometer. Shown by the dashed line is the bandpass of the MLM array. The bright unlabeled lines belong to Ti VI–Ti VIII.

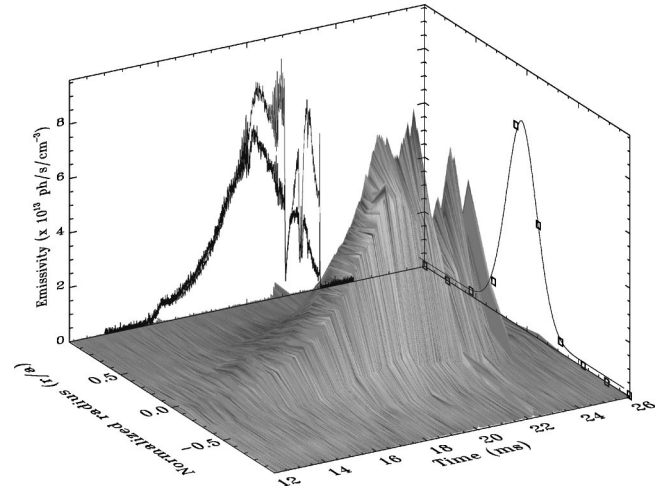

FIG. 5. The emissivity of the λ150 O VI line. Two internal reconnection events occur at $t \simeq 22$ ms and $t \simeq 23$ ms. Side panels show time histories of two central channels and an example of a fitted profile measured at $t = 21.8$ ms. Same discharge as in Fig. 6.

plasma is shown in Fig. 2 (b). The array is enclosed in a modified four inch stainless steel tube. The problem of light reflection inside the chamber was not specifically addressed. The tests with a 500 W tungsten lamp demonstrated that internal reflections may contribute less than 3% of the signal. The array operates in two modes: the radiated power measurement mode, with a clear aperture of 0.65 cm $\times$2.0 cm between the diodes and the plasma, and the filtered mode, with a 3 kÅ Ti filter or a 5 kÅ Be filter. The calculated filter transmission[19] is given in Fig. 4. The Ti and Be filters are used to transmit predominantly the 41 Å C V emission and the O VI XUV line emission, respectively. The etendue of each channel is 2×10^{-3} cm^2 rad.

Data inversion is performed using an algebraic inversion algorithm, assuming toroidal symmetry of the shells with equal emissivity. The ith chord-integrated brightness (irradiance) B_i is given by $B_i = \Sigma_j \epsilon_j l_{ij}$, where ϵ_j is the jth shell emissivity, l_{ij} is the length of the ith chord in the jth shell and is determined from geometrical considerations (Fig. 2). The inverted emissivity is given by $\epsilon_j = \Sigma_i l_{ij}^{-1} B_i$, and the inverse length matrix l_{ij}^{-1} is calculated only once.

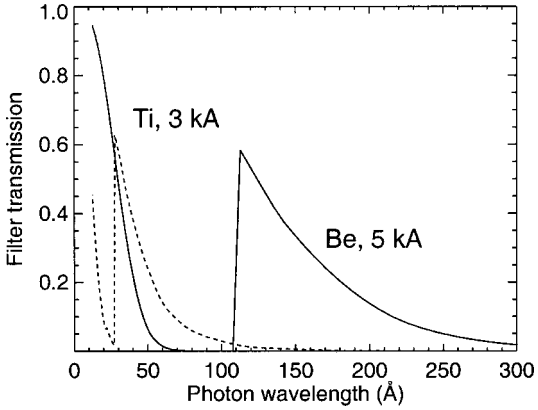

FIG. 4. Calculated transmission of the 5 kÅ Be filter and 3 kÅ Ti filter.

C. Detectors, amplifiers, data acquisition

The photodiodes AXUV-SP2 from International Radiation Detectors are used. The diode area exposed to radiation is about 1 cm^2. Each photodiode is enclosed in a Faraday cage holder with a 40 μm diameter Ni mesh on the front for protection from high frequency electromagnetic pickup. Semi-rigid coaxial cable with SMA connectors is used inside the vacuum. Amplifiers are attached directly on the feedthroughs on the air side of the vacuum chamber. Custom-built DC-coupled 120 kHz 10^7 gain amplifiers, biased at -5 V, are used with the MLM array. The foil filter array is equipped with 50 kHz AC-coupled amplifiers.[4] Amplified signals are digitized by the CAMAC 8210 LeCroy digitizers at 250 kHz and recorded to disk via a GPIB-interfaced computer running LabView software.

III. PERFORMANCE ON CDX-U SPHERICAL TOKAMAK

A. Impurity profile measurements

Spectrally filtered AXUV diodes are especially useful for soft x-ray and XUV absolute brightness measurements. Figures 5 and 6 show inverted emissivity profiles of O VI and C V, respectively. The emissivity profiles are modeled using the collisional-radiative code CRMLIN and the 1D impurity transport code MIST.[20] The measured T_e and n_e profiles (Sec. I) are used as inputs. The modeling[11] demonstrates that diffusion coefficients in the range 2000–5000 cm^2/s and a large inward convection velocity is necessary to reproduce the measured profiles. Impurity concentrations and the Z_{eff} profiles are also derived. After several months of continuous plasma operations and titanium gettering between discharges, both carbon and oxygen central concentrations were brought down to 1–2%. The Z_{eff} profiles are peaked, and in the core $Z_{\mathrm{eff}} \simeq 1.7-2$.

B. Plasma imaging and radiated power measurements

The plasma emissivity profile for a typical CDX-U discharge is shown in Fig. 7. The AXUV diode sensitivity of

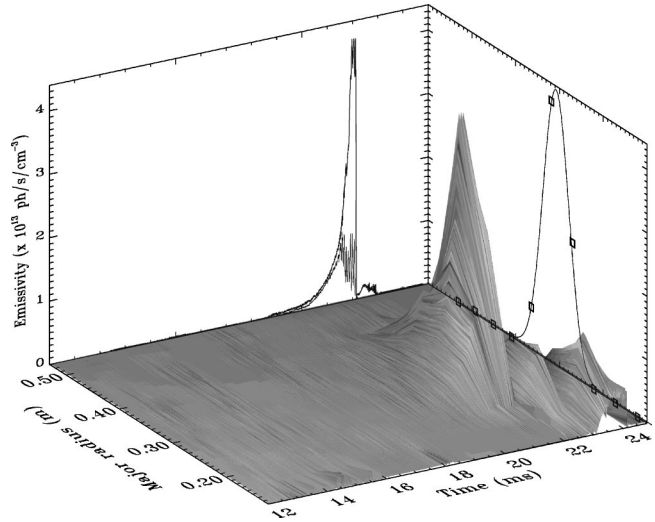

FIG. 6. Soft x-ray emissivity (mostly λ41 C V) obtained from the FFR array with a Ti filter. Side panels show time histories of two central channels and an example of a fitted profile measured at $t=21.8$ ms. Two internal reconnection events occur at $t\simeq 22$ ms and $t\simeq 23$ ms.

0.25 A/W is used for absolute power calibration. However, the application of AXUV diodes as bolometers (radiometers) is justified only for plasma radiation with $E_{\mathrm{phot}}\geqslant 200$ eV. This is demonstrated in Fig. 8. Major core impurity radiators in CDX-U are O VI and C V. Whereas C V radiates predominantly in the XUV range, the major fraction of O VI line radiated power is in the far ultraviolet range, due to the λ1034 line. The AXUV diode sensitivity at λ1034 is $\simeq 0.127$ A/W. Thus, the diode response (in units of current per plasma electron per photon) $\eta = L_{\mathrm{OVI}}\times\epsilon$ is overestimated. Here L_{OVI} is radiative power loss coefficient in units of $\mathrm{W\,cm^3}$ and $\epsilon = 0.25$ A/W is average diode sensitivity. The corrected response $\eta_{\mathrm{corr}} = \Sigma_\lambda L_\lambda \times \epsilon_\lambda$ is about a factor of 2 smaller, and the true radiated power is about a factor of 2 greater. Spectrally resolved power and AXUV sensitivity corrected cooling curve calculations are underway for low and medium Z elements for different $n_e\tau$ parameters, where n_e is electron temperature and τ is ion residence time. The $n_e\tau$ parameter is used to account for impurity transport,

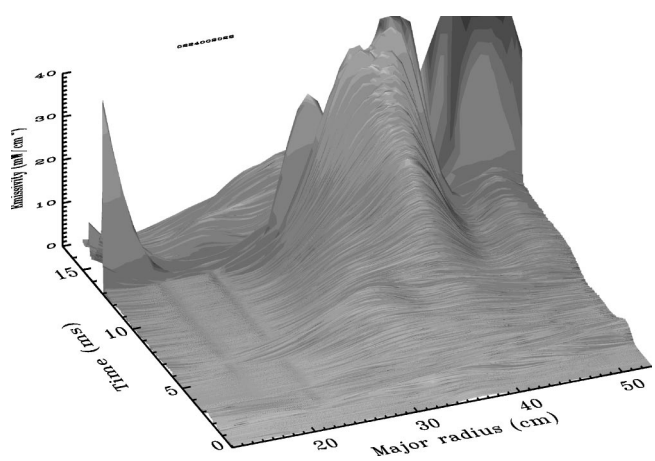

FIG. 7. Plasma emissivity of a typical CDX-U discharge. An internal reconnection event occurs at $t=13$ ms.

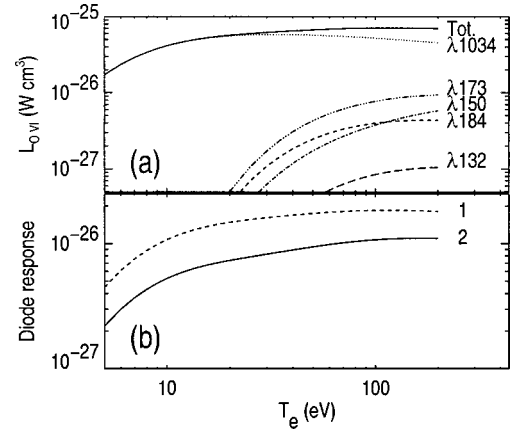

FIG. 8. (a) O VI spectrally resolved radiative power loss coefficient L_{OVI}, (b) calculated diode response η using average sensitivity $\epsilon = 0.26$ A/W (curve 1) and the spectrally resolved accounting with ϵ_λ (curve 2).

which shifts the coronal equilibrium cooling curves towards higher temperatures. In CDX-U, measurements of several extreme and far ultraviolet impurity lines allow us to do full power accounting. The fraction of radiated power in CDX-U is typically 10–20% of the ohmic input power. The input power is estimated to be 60–120 kW either using the Spitzer expression for plasma resistivity for the CDX-U range of Z_{eff}, I_p, and T_e or from the measured I_p and V_{loop}. The foil filter array also proved to be very useful for plasma dynamics observations. In Fig. 7, the discharge breakdown at $t=1$ ms and plasma position are clearly seen. A local emissivity peak at $t\simeq 7$ ms and $R=0.34$ m is due to the C IV emission. Later in the discharge, C IV burns through and only O VI and C V are present in the core.

C. MHD instabilities in CDX-U

Impurity line emission has been previously used on CDX-U for MHD mode identification.[4–8] The MHD modes observed presently in CDX-U include the saw-tooth oscillations, low n, m modes and internal reconnection events (IREs). The saw-tooth period is $\tau_{\mathrm{st}}\simeq 300$ μs, and the inversion radius is about 4 cm. These parameters are inferred from both the radiated power and the C V profiles, measured by the SBD array. Transfer of the absolute calibration from the FFR array to the SBD array will allow ΔT_e estimates in the saw-tooth crashes. The low n, m modes are frequently observed in CDX-U discharges prior to the IRE. The spectroscopic signatures of the IRE are emissivity collapse (Fig. 6), due to plasma pressure collapse, and rapid expulsion of plasma from the core, which results in emissivity spreading (e.g., Fig. 7). The observed MHD instabilities do not affect the measured impurity profiles and the derived transport parameters.

D. Discussion

Impurity accumulation has been previously observed in CDX-U and attributed to the neoclassical impurity accumulation instability.[6] The two main impurities, carbon and oxygen, are in the Pfirsch–Schluter regime in CDX-U, with fairly high concentrations in the core. Enhanced impurity

convection due to impurity radiative cooling and the associated neoclassical temperature screening effect failure is the driving mechanism of the saturated instability.[21] However, the radiated power estimates obtained from the AXUV radiometer array measurements in the 1999–2000 run campaign demonstrated that the radiated power fraction is not sufficient to trigger the accumulation instability. An alternative mechanism is considered in order to explain the observed impurity peaking. It retains the neoclassical nature of the impurity transport the ion density gradients is responsible for the enhancement of the convection inward impurity flow.

IV. CONCLUSIONS

Two AXUV diode arrays are used on CDX-U spherical torus for intrinsic O VI and C V profile measurements, radiated power estimates and observations of MHD instabilities. The incidence geometry of the Mo/B_4C mirrors used as dispersive elements can be easily modified to allow measurements of line brightness profiles in the range between 90 and 200 Å. In the near future, following the change in the CDX-U research program towards the liquid lithium limiter (L3) experiments,[22] the MLM array will be re-tuned for the 135 Å $(1s\,^2S-2p\,^2P)$ Li III emission. With the exception of a weak $\lambda 132$ $(2p-4s)$ O VI line, the spectral region in the vicinity of 135 Å within the MLM bandpass $\Delta\lambda$ is free from intrinsic impurity line emission (Fig. 3).

ACKNOWLEDGMENTS

We thank Mr. J. Taylor (PPPL) for his technical assistance. This work is supported by U.S. DoE Grant No. DE-FG02-86ER53214 at The Johns Hopkins University and U.S. DoE Contract No. DE-AC02-76CH03073 at Princeton Plasma Physics Laboratory.

[1] R. S. Korde and L. R. Canfield, Proc. SPIE **1140**, 126 (1989).
[2] R. L. Boivin, J. A. Goetz, E. S. Marmar, J. E. Rice, and J. L. Terry, Rev. Sci. Instrum. **70**, 260 (1999).
[3] A. Alekseyev, G. Petrov, A. Kurnosov, A. Chernoby, A. Amosov, D. Portnov, A. Bolov, and R. Korde, Plasma Devices Op. **7**, 139 (1999).
[4] D. Stutman, J. Menard, Y. S. Hwang, W. Choe, M. Ono, M. Finkenthal, V. Soukhanovskii, M. J. May, S. P. Regan, and H. W. Moos, Rev. Sci. Instrum. **68**, 1059 (1997).
[5] D. Stutman, Y. S. Hwang, J. Menard, W. Choe, M. Ono, M. Finkenthal, M. J. May, S. P. Regan, V. Soukhanovskii, and H. W. Moos, Rev. Sci. Instrum. **68**, 1055 (1997).
[6] D. Stutman, M. Finkenthal, V. Soukhanovskii, M. J. May, H. W. Moos, and R. Kaita, Rev. Sci. Instrum. **70**, 572 (1999).
[7] M. Ono, D. Stutman, Y. S. Hwang, W. Choe, J. Menard, T. Jones, E. Lo, R. Amstrong, M. Finkenthal, V. Gusev, S. Jardin, R. Kaita, J. Manickam, T. Munsat, R. Nazikian, and Y. Petrov, *16th IEAE Conference IEAE-CN-64/C2-2* (IEAE, Montreal, Canada, 1996).
[8] D. Stutman, M. Finkenthal, V. Soukhanovskii, J. Menard, T. Munsat, R. Kaita, and R. Majeski, Plasma Phys. Controlled Fusion **41**, 867 (1999).
[9] J. Menard, R. Majeski, R. Kaita, M. Ono, T. Munsat, D. Stutman, and M. Finkenthal, Phys. Plasmas **6**, 2002 (1999).
[10] P. C. Efthimion, J. C. Hosea, R. Kaita, R. Majeski, and G. Taylor, Rev. Sci. Instrum. **70**, 1018 (1999).
[11] V. A. Soukhanovskii, D. Stutman, M. Iovea, M. Finkenthal, H. W. Moos, D. Hoffman, T. Munsat, J. Menard, R. Majeski, R. Kaita, B. Jones, J. Spaleta, G. Taylor, and P. Efthimion, Bull. Am. Phys. Soc. **44**, 268 (1999).
[12] T. Munsat and B. Leblanc, Rev. Sci. Instrum. **70**, 755 (1999).
[13] C. B. Forest, G. Greene, and M. Ono, Rev. Sci. Instrum. **61**, 2888 (1990).
[14] J. E. Menard, Ph.D. thesis, Princeton University, 1998.
[15] G. Taylor, P. Efthimion, B. Jones, T. Munsat, J. Spaleta, J. Hosea, R. Kaita, R. Majeski, and J. Menard, Rev. Sci. Instrum. (these proceedings).
[16] A. P. Zwicker, S. P. Regan, M. Finkenthal, H. W. Moos, E. B. Soloman, R. Watts, and J. R. Roberts, Appl. Opt. **29**, 3694 (1990).
[17] S. Tsuji, Y. Nagayama, K. Kawahata, N. Noda, and S. Tanahashi, Nucl. Fusion **22**, 1082 (1982).
[18] Y. Nagayama and A. W. Edwards, Rev. Sci. Instrum. **63**, 4757 (1992).
[19] The Center for X-ray Optics, Lawrence Berkeley National Laboratory, http://www.cxro.lbl.gov
[20] R. A. Hulse, Nucl. Technol./Fusion **3**, 259 (1983).
[21] M. Z. Tokar', J. Rapp, G. Bertschinger, L. Konen, H. R. Koslowski, A. Kramer-Flecken, V. Phillips, U. Samm, and B. Unterberg, Nucl. Fusion **37**, 1691 (1997).
[22] R. Kaita, P. Efthimion, D. Hoffman, B. Jones, H. Kugel, R. Majeski, T. Munsat, S. Raftopoulos, G. Taylor, J. Timberlake, V. Soukhanovskii, D. Stutman, M. Iovea, M. Finkenthal, R. Doerner, S. Luckhardt, R. Maingi, and R. Causey, Rev. Sci. Instrum. (these proceedings).